Modified Schwarzschild imaging spectrometer with a low *F*-number and a long slit

Qingsheng Xue

Changchun Institute of Optics, Fine Mechanics and Physics, Chinese Academy of Sciences, Changchun, Jilin 130033, China (qshxue2006@163.com)

Received 17 July 2013; revised 2 September 2013; accepted 4 September 2013; posted 5 September 2013 (Doc. ID 194069); published 30 September 2013

A modified Schwarzschild imaging spectrometer utilizing three nonconcentric aspheric mirrors and a plane grating is designed that can handle low *F*-number, long slit, and broad spectral range. Based on the geometrical aberration theory and Rowland circle condition, the astigmatism-correcting method of the Schwarzschild imaging spectrometer is analyzed. The design procedure of initial parameters is programmed using Matlab software. As an example, a modified Schwarzschild imaging spectrometer operating in 400–1000 nm waveband with *F*-number of 2.5 and slit length of 13 mm is designed, and good imaging quality is obtained. © 2013 Optical Society of America

OCIS codes: (300.0300) Spectroscopy; (300.6190) Spectrometers; (120.4570) Optical design of instruments; (120.0120) Instrumentation, measurement, and metrology; (120.0280) Remote sensing and sensors.

http://dx.doi.org/10.1364/AO.52.006956

1. Introduction

Imaging spectrometers are novel optical instruments that combine conventional imaging with spectroscopy to record the spectrum of every point in a scene. The data provided by the instrument can be used for a wide range of purposes, spanning many applications in research and industry [1,2]. The modified Czerny–Turner mount [3,4] and Offner mount [5,6] are two of the most popular optical configurations applied to build imaging spectrometers. The modified Czerny–Turner imaging spectrometers using a plane grating have some advantages, such as easy fabrication and low cost. However, the *F*-number of modified Czerny–Turner imaging spectrometers is high, higher than $f/5$, so the throughput is low. The Offner imaging spectrometers using a convex grating have some advantages, such as low *F*-number ($f/3$), long slit, and low distortions, so the throughput is high. However, the fabrication of the convex grating is more difficult than that of the plane grating, the price of the convex grating is higher than that of the plane grating, and the diffraction efficiency of the convex grating is less than that of the plane grating. A Schwarzschild spectrometer utilizing double Schwarzschild optical systems and a plane grating was suggested and demonstrated in [7]. Here, each Schwarzschild optical system was composed of two concentric spherical mirrors. However, its *F*-number is only $f/4$, the slit length is only 4 mm, and the distortions were not demonstrated. Some applications (such as remote sensing of coastal environment and atmosphere) require high throughput, long slit, wide waveband, low spectral distortion known as smile, and low spatial distortion known as keystone [8,9]. In this paper, astigmatism removal is analyzed based on the geometrical aberration theory and Rowland circle condition. In Section 2, we derive the conditions that remove astigmatism. In Section 3, we program a design procedure calculating the initial structural parameters. In Section 4, we present a ray-tracing analysis of such a design. A summary is given in Section 5.

2. Astigmatism-Correcting Condition

In this section we derive the astigmatism-correcting condition based on the geometrical aberration theory

1559-128X/13/286956-06$15.00/0

and Rowland circle condition. The Rowland circle was first defined for spherical grating by Beulter [10], as a circle of diameter R (R being the grating curvature radius), which is tangent to the grating at the chief ray incidence point and is contained within a plane perpendicular to the grating grooves. As shown in Fig. 1, It has two interesting properties that are fulfilled every time the object point is located on this circle. First, the meridional image is located on the same circle, regardless of wavelength, and second, the coma aberration corresponding to this image is null. According to the theory of concave grating, the imaging relations can be written as

$$\frac{\cos^2\theta}{r}+\frac{\cos^2\theta'}{r'_M}=\frac{\cos\theta+\cos\theta'}{R}, \tag{1}$$

$$\frac{1}{r}+\frac{1}{r'_S}=\frac{\cos\theta+\cos\theta'}{R}, \tag{2}$$

where R is the grating curvature radius, r is the objective distance, r'_M is the meridional image distance, r'_S is the sagittal image distance, θ is the incident angle to concave grating, and θ' is the diffraction angle of concave grating. The grating law can be written as

$$\sin\theta+\sin\theta'=mg\lambda, \tag{3}$$

where m is diffraction order, g is grating density, and λ is wavelength. According to Eq. (3), when $m=0$, $\theta=-\theta'$, a concave grating can be considered as a concave spherical mirror. Equations (1) and (2) can be rewritten as

$$\frac{1}{r}+\frac{1}{r'_M}=\frac{2}{R\cos\theta}, \tag{4}$$

$$\frac{1}{r}+\frac{1}{r'_S}=\frac{2\cos\theta}{R}. \tag{5}$$

If the object point is on a Rowland circle of the mirror, i.e., $r=R\cos\theta$, the meridional image distance can be derived from Eq. (4) as

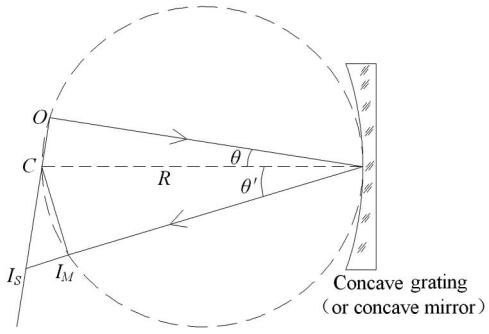

Fig. 1. Schematic diagram of Rowland circle.

$$r'_M=R\cos\theta. \tag{6}$$

Therefore, the meridional image point is also on a Rowland circle of the mirror. The sagittal image distance can be derived from Eq. (5) as

$$r'_S=\frac{R\cos\theta}{\cos 2\theta}, \tag{7}$$

therefore, the sagittal imaging point of the mirror on the line through an object point and the curvature center of the mirror. The difference in astigmatic foci yielded by the mirror can be derived as

$$\Delta l'=r'_S-r'_M=\left(\frac{1}{\cos 2\theta}-1\right)R\cos\theta. \tag{8}$$

The schematic diagram of initial configuration of the Schwarzschild imaging spectrometer is shown in Fig. 2. First, the rays from the slit are collimated by a Schwarzschild optical system; then, the rays are diffracted by the plane grating; finally, the rays are focused on the image plane by another Schwarzschild optical system. Collimating and focusing are both done by Schwarzschild optical systems, so the astigmatism removal condition is only analyzed in the collimator. The schematic diagram of the Schwarzschild collimator is shown in Fig. 3. The object point is on a Rowland circle of Mirror 1. Therefore

$$r_1=R_1\cos\theta_1, \tag{9}$$

where θ_1 is the incident angle to the Mirror 1, and R_1 is the curvature radius of Mirror 1. According to Eq. (8), the astigmatism yielded by Mirror 1 can be written as

$$\Delta l'_1=\left[\frac{1}{\cos(2\theta_1)}-1\right]R_1\cos\theta_1. \tag{10}$$

Based on Eq. (4), the virtual object distance of Mirror 2 for meridional rays r'_{M2} can be written as

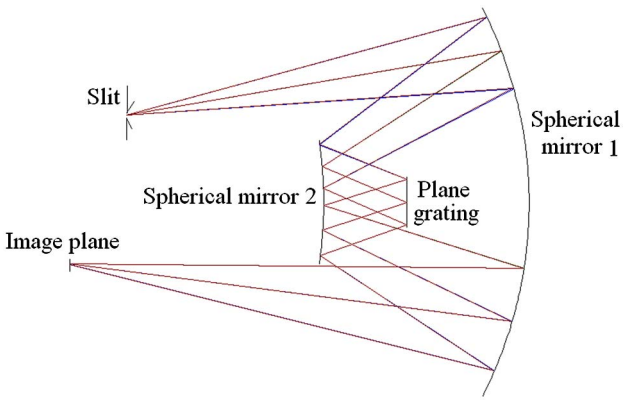

Fig. 2. Schematic diagram of initial configuration for Schwarzschild spectral imaging system.

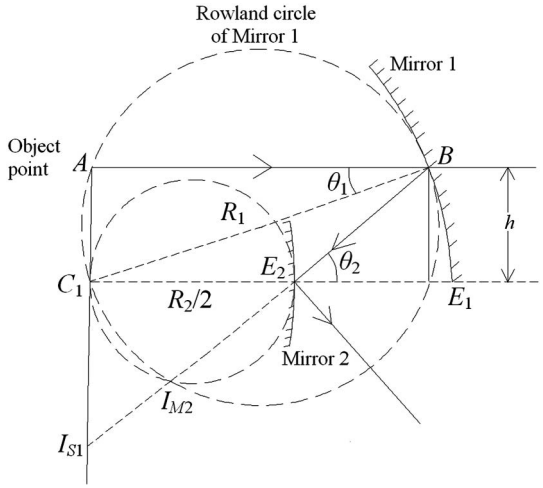

Fig. 3. Program block diagram for calculating the initial structural parameters.

$$r'_{M2} = (R_2/2)\cos\theta_2, \tag{11}$$

where R_2 is the curvature radius of Mirror 2 and θ_2 is the incident angle to the Mirror 2. The astigmatism yielded by Mirror 2 can be written as

$$\Delta l'_2 = (R_2/2)\left[\cos\theta_2 - \frac{1}{\cos\theta_2}\right]. \tag{12}$$

Based on the geometrical relations, the incident angles θ_1 and θ_2 satisfy

$$\theta_2 = 2\theta_1. \tag{13}$$

The off-axis distance h can be written as

$$h = R_1 \sin\theta_1. \tag{14}$$

The difference in astigmatic foci yielded by the two spherical mirrors of the Schwarzschild optical system can be derived as

$$\Delta l'_{12} = \Delta l'_1 + \Delta l'_2 = \left[\frac{1}{\cos(2\theta_1)} - 1\right]R_1\cos\theta_1 + (R_2/2)\left[\cos\theta_2 - \frac{1}{\cos\theta_2}\right]. \tag{15}$$

If $\Delta l'_{12} = 0$, the astigmatism is removed. According to Eq. (15), we derive the astigmatic removal condition as

$$R_2 = \frac{2R_1\sin\theta_1}{\sin\theta_2} = R_1/\cos\theta_1. \tag{16}$$

Obviously, in our design, the two spherical mirrors are not concentric. Based on sine theorem, we derived the distance between the curvature center of Mirror 1 and the vertex of Mirror 2 as

$$|C_1E_2| = \frac{R_1\sin\theta_1}{\sin\theta_2} = R_2/2. \tag{17}$$

Therefore, the distance between the vertex of Mirror 1 and the vertex of Mirror 2 is written as

$$d_1 = R_1 - R_2/2 = \frac{R_1(2\cos\theta_1 - 1)}{2\cos\theta_1}. \tag{18}$$

The total focal length of Mirror 1 and Mirror 2 can be derived as

$$f' = \frac{f'_1 f'_2}{f'_1 + f'_2 - d_1}, \tag{19}$$

where the $f'_1 = -R_1/2$ is the focal length of Mirror 1 and $f'_2 = -R_2/2$ is the focal length of Mirror 2. Substituting Eqs. (16) and (18) into Eq. (19) yields

$$f' = \frac{R_1}{2\cos\theta_1}. \tag{20}$$

The plane grating law is rewritten as

$$\sin\alpha + \sin\beta = m\lambda g, \tag{21}$$

where, α is the incident angle to the plane grating and β is the diffractive angle of plane grating. By differentiating Eq. (21) with respect to λ, we obtain

$$\frac{d\beta}{d\lambda} = \frac{mg}{\cos\beta}. \tag{22}$$

The dispersive width on the image plane for wavelengths from λ_1 to λ_2 can be written as

$$\Delta p = f' \cdot \frac{mg}{\cos\beta} \cdot (\lambda_2 - \lambda_1). \tag{23}$$

3. Design Procedure

The basic parameters of a Schwarzschild imaging spectrometer are waveband $\lambda_1 \sim \lambda_2$, the F-number $F/\#$, the slit length $2L$, and the dispersive width Δp. First, we choose the diffractive order m, grating density g, and the diffractive angle β. The total focal length f' can be determined based on Eq. (23), and the incident angle α to the plane grating can be determined by Eq. (21). Then we choose the incident angle θ_1; the radius of Mirror 1 R_1 can be derived from Eq. (20). Finally, the off-axis distance h can be derived from Eq. (14), the radius R_2 can be derived from Eq. (16), and d_1 can be derived from Eq. (18). Thus, all the structural parameters can be obtained. We programmed the procedure, calculating the initial parameters, in MATLAB. The program block diagram is shown in Fig. 4.

4. Ray-Tracing Analysis

In this section, we present a design example to illustrate the performance of the Schwarzschild imaging

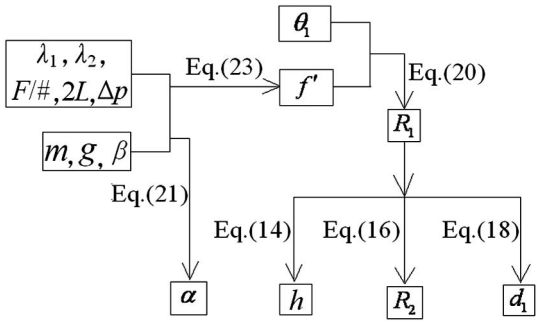

Fig. 4. Program block diagram for calculating the initial structural parameters.

spectrometer. We calculate initial structural parameters using the procedure presented previously, and then model and analyze this system using the optical system design program ZEMAX [11].

The imaging spectrometer is designed to sounding coastal ocean with a low F-number and a broad spectral range from 400 to 1000 nm, i.e., the wavelength λ_1 is 400 nm, λ_2 is 1000 nm, and the central wavelength λ_c is 700 nm. The F number is 2.5, the slit length $2L$ is 13 mm, and the dispersive width Δp is 12 mm. A CCD produced by E2V company with a size of 13.3 mm × 13.3 mm (pixel size is 13 μm × 13 μm, and pixel number is 1024 × 1024) is chosen. We select an off-the-shelf plane grating. The groove density is 150 grooves/mm, the diffractive order m is 1, the diffractive angle β is 38° for the central wavelength λ_c, and the incident θ_1 is 15°. The basic parameters of the spectrometer are summarized in Table 1. From these we calculated f', α, R_1, R_2, h, d_1, using the procedure in Section 3, to give the values in Table 2. We optimize the Schwarzschild imaging spectrometer based on the initial parameters in Table 2 by using the merit function of ZEMAX. To improve the image quality, Mirror 1 and Mirror 2 are aspherizing. The curvature radius of the mirrors and distances between optical elements and k_i of the aspheric mirrors in Eq. (24) can be selected as variables for the optimization

$$z = \frac{cr^2}{1 + \sqrt{(1 - (1 + k_i)c^2r^2)}}, \tag{24}$$

Table 1. Imaging Spectrometer Basic Parameters

Parameter	Value
λ_c (nm)	700
λ_1 (nm)	400
λ_2 (nm)	1000
$F/\#$	2.5
L (mm)	6.5
Δp (mm)	12
g (g/mm)	150
M	1
β (°)	38
θ_1 (°)	15

Table 2. Imaging Spectrometer Designed Parameters

Specifications	Initial Parameter	Optimized Parameter
α (°)	30.708	30.708
f' (mm)	105.068	105.068
R_1 (mm)	202.976	202.976
R_2 (mm)	210.136	214.546
R_3 (mm)	202.976	201.058
h (mm)	52.534	52.534
d_1 (mm)	97.908	97.908
k_1	0	0.14182
k_2	0	2.70830
k_3	0	0.15725

where z is the sag of the surface parallel to the optical axis, c is the curvature of the aspheric mirror, and k_i ($i = 1, 2, 3$) is the conic coefficient. 0, 1.3, 3.25, 5.2, and 6.5 mm positions from the center of the line slit are selected as field positions. The optimized parameters are summarized in Table 2. Figure 5 shows the layout of the optimized system, which is composed of three different aspheric mirrors and the plane grating.

With the help of ZEMAX, the optical performance of the system can be predicted and plotted. Spot diagrams at the detector surface are calculated for different wavelengths and different fields of view at the entrance slit. Figure 6 shows the geometrical spot diagrams of the optimized system for 400, 500, 600, 700, 800, 900, and 1000 nm, and 0, 1.3, 3.25, 5.2, and 6.5 object positions from the center of the line slit parallel to axis x, and the 13 μm × 13 μm box for comparison. The optimized system has spot size less than 13 μm as shown in Fig. 6. To show the result of aberration correction for broadband spectral simultaneity, root mean square (RMS) spot radius is given as a function of wavelength for the modified Schwarzschild imaging spectrometers (utilizing three nonconcentric aspheric mirrors) and the existing Schwarzschild imaging spectrometer (utilizing three concentric spherical mirrors). Obviously, the RMS spot radius is less than 2.5 μm over the broad working wavelength band from 400 to

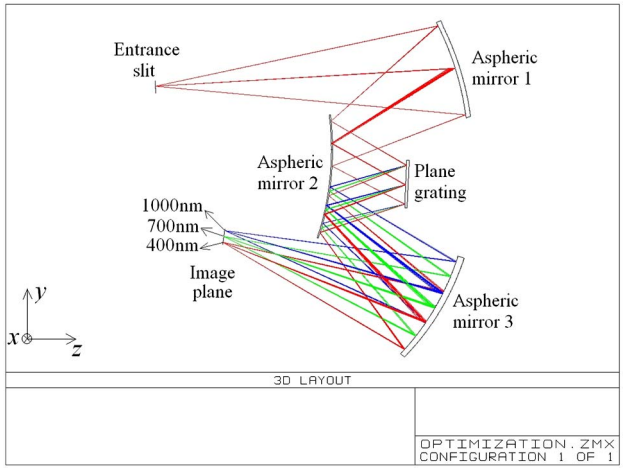

Fig. 5. Layout of Schwarzschild spectral imaging system.

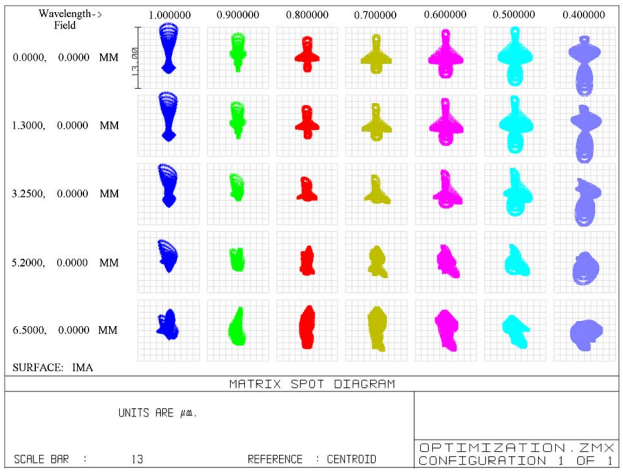

Fig. 6. Spot diagram of Schwarzschild spectral imaging system.

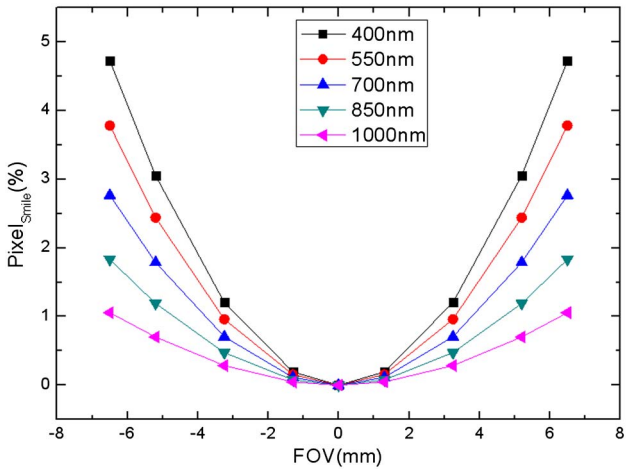

Fig. 8. Total smile for different wavelengths.

1000 nm for our modified Schwarzschild imaging spectrometer, as shown in Fig. 7(a). The results demonstrate that aberration is simultaneously corrected over a broad spectral range. However, the RMS spot radius is larger than 30 μm, resulting from the devastating astigmatism for the existing Schwarzschild imaging spectrometer, as shown in Fig. 7(b).

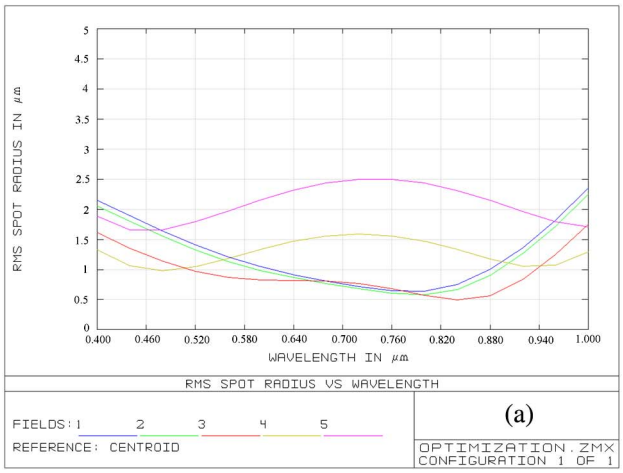

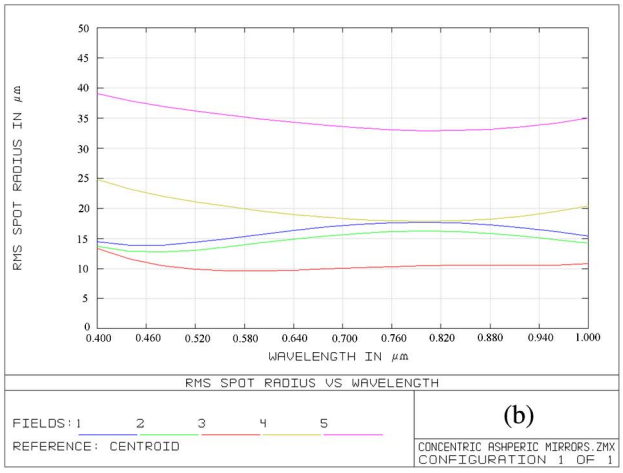

Fig. 7. RMS spot radius versus wavelength for (a) the modified Schwarzschild imaging spectrometer utilizing three nonconcentric aspheric mirrors and (b) the existing Schwarzschild imaging spectrometers utilizing three concentric spherical mirrors.

Spatial and spectral uniformity are essential properties of any imaging spectrometer. For an accurate acquisition of hyperspectral data, typical distortion requirements go down to 20% or even 10% of a pixel. Figure 8 shows the total smile for different wavelengths. The total smile is symmetrical about center of slit, and increases when the wavelengths become longer. However, the total smile is less than 5% of a pixel. Figure 9 shows the keystone for different object heights. The keystone is increased when the object height is higher. For a same object height, the keystone of the marginal wavelength is larger than that of the central wavelength. The keystone is less than the 2% of a pixel. The results satisfy the application requirement and demonstrate that good imaging quality is simultaneously obtained over the broad wavelength region with a low F-number and long slit.

5. Summary

We have proposed and designed a modified Schwarzschild imaging spectrometer with a low F-number, long slit, and a broad spectral range,

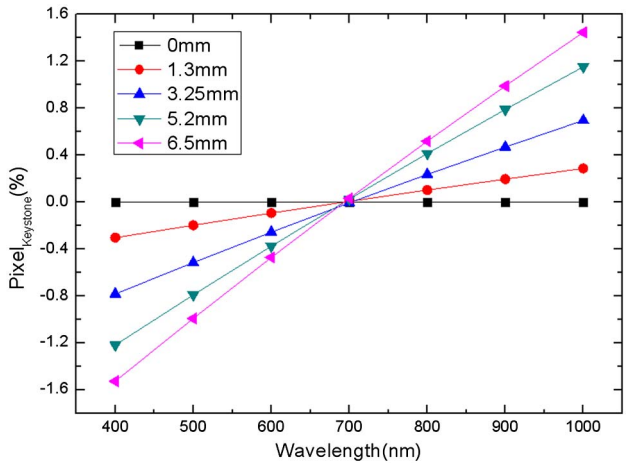

Fig. 9. Keystone for different object heights.

which is composed of three nonconcentric aspheric mirrors and the plane grating. The aspheric mirrors and the plane grating are easy to make and not expensive. We derive a design method of correcting astigmatism based on geometrical aberration theory and the Rowland concept. In doing so, high-optical-performance imaging spectrometers are designed even for low F-number, long slit, and broad spectral range. RMS spot radius less than 2.5 μm are obtained for speed as high as $f/2.5$, slit length of 13 mm, and spectral ranges of 400–1000 nm. This design will be useful for coastal ocean sounding, and will have broad applications in atmospheric sounding and in studying the spatially resolved ultrashort pulse characterization.

The work described in this paper is supported by the National Natural Science Foundation of China (NSFC) under grant 41105014.

References

1. H. A. Bender, P. Mouroulis, R. O. Green, and D. W. Wilson, "Optical design, performance and tolerancing of next-generation air borne imaging spectrometers," Proc. SPIE **7812**, 78120P (2010).
2. X. Prieto-Blanco, C. Montero-Orille, H. González-Núñez, M. D. Mouriz, E. L. Lago, and R. de la Fuente, "The Offner imaging spectrometer in quadrature," Opt. Express **18**, 12756–12769 (2010).
3. Q. Xue, S. Wang, and F. Lu, "Aberration-corrected Czerny–Turner imaging spectrometer with a wide spectral region," Appl. Opt. **48**, 11–16 (2009).
4. D. R. Austin, T. Witting, and I. A. Walmsley, "Broadband astigmatism-free Czerny–Turner using spherical mirrors," Appl. Opt. **48**, 3846–3853 (2009).
5. S. H. Kim, H. J. Kong, H. Ku, and J. H. Lee, "Analytical design of a hyper-spectral imaging spectrometer utilizing a convex grating," Proc. SPIE **8515**, 85150V (2012).
6. X. Prieto-Blanco, C. Montero-Orille, B. Couce, and R. de la Fuente, "Analytical design of an Offner imaging spectrometer," Opt. Express **14**, 9156–9168 (2006).
7. M. D. Mouriz, E. L. Lago, X. Prieto-Blanco, H. González-Núñez, and R. de la Fuente, "Schwarzschild spectrometer," Appl. Opt. **50**, 2418–2424 (2011).
8. J. Fisher, J. Antoniades, C. Rollins, and L. Xiang, "A hyperspectral imaging sensor for the coastal environment," Proc. SPIE **3115**, 179–185 (2000).
9. P. Mouroulis, R. O. Green, and D. W. Wilson, "Optical design of a coastal ocean imaging spectrometer," Opt. Express **16**, 9087–9096 (2008).
10. H. Beutler, "The theory of concave grating," J. Opt. Soc. Am. **35**, 311–350 (1945).
11. ZEMAX is a trademark of Zemax development Corporation, Bellevue, Washington 98004, USA.